

ANALYTICAL TEST STRUCTURE MODEL FOR DETERMINING LATERAL EFFECTS OF TRI-LAYER OHMIC CONTACT BEYOND THE CONTACT EDGE

**Neelu Shrestha, Geoffrey K. Reeves, Patrick W. Leech, Yue Pan,
Anthony S. Holland**

School of Engineering, RMIT University, Melbourne, Victoria, Australia

Abstract. *Contact test structures where there is more than one non-metal layer, are significantly more complex to analyse compared to when there is only one such layer like active silicon on an insulating substrate. Here, we use analytical models for complex test structures in a two contact test structure and compare the results obtained with those from Finite Element Models (FEM) of the same test structures. The analytical models are based on the transmission line model and the tri-layer transmission line model in particular, and do not include vertical voltage drops except for the interfaces. The comparison shows that analytical models for tri-layer contacts to dual active layers agree well with FEM when the Specific Contact Resistances (SCR) of the contact interfaces is a significant part of the total resistance. Overall, there is a broad range of typical dual-layer-to-TLTM contacts where the analytical model works. The insight (and quantifying) that the analytical model gives on the effect of the presence of the contact, on the distribution of current away from the contact is shown.*

Key words: *Ohmic contact, specific contact resistance, transfer length, Transmission Line Model*

1. INTRODUCTION

The study of specific contact resistivity (ρ_c , [$\Omega \cdot \text{cm}^2$]), one of the most important parameters to investigate metal semiconductor interfacial properties, has been reported using several test structures [e.g. 1-6]. The effect of this parameter on the resistance of device components is also an area of investigation and an example is the effect of interfaces in via liners [7]. The transmission line model (TLM) is the commonly used among them and was first applied for analysing/determining the resistance components of semiconductor ohmic contacts, by Shockley in 1964 [5]. For many years the TLM test structure was considered accurate for contacts such as Aluminium to Silicon. A more complex TLM model for contacts such as alloyed Ni/Ge/Au to GaAs was introduced by

Received September 26, 2016; received in revised form November 16, 2016

Corresponding author: Neelu Shrestha

School of Engineering, RMIT University, Melbourne, Victoria, Australia

(E-mail: neelu_shrestha@hotmail.com)

Reeves [6]. The example given has a metal, an alloyed and a semiconductor layer. Another example of a tri-layer contact structure is Aluminium-silicide–Silicon. The analytical models due to the dual-layer and tri-layer structures considered the contact as beginning at the leading edge of the metal. Yao Li [8] developed an analytical model to show (and quantify) how the presence of the contact affects the current (and hence voltage distribution) away from the leading edge. This was also investigated by Reeves [9]. The works in these references [6, 8, 9] were combined in the investigation for this paper and their utilisation and further demonstration of accuracy is demonstrated. The analytical model demonstrated in this paper can provide a solution to the 2L-TLM, contact structure (a metal contact to a dual semiconductor layer (see Fig. 1(a))), considered intractable in 1994 [10].

For most semiconductor devices the sheet resistance of the semiconductor active layer is sufficient to quantify its resistive effect even for typical planar contacts such as source/drain contacts. The principle of the TLM models for ohmic contacts relies on this being so. Only in cases where the specific contact resistance of the metal/semiconductor interface is extremely small, there will be significant vertical voltage drop in the semiconductor layer. TLM models (analytical type models) do not account for vertical voltage drop in the semiconductor layer but FEM models do. This paper investigates the difference.

FEM is a powerful technique and is used here to demonstrate the accuracy of the analytical models which are also expanded here to demonstrate their usefulness as one approach to quantifying the total resistance encountered by current between two Tri-layer contacts to a dual-layer (parallel sheet resistances) structure as shown in Fig 1(a) and the corresponding resistor network model shown in Fig 1(b).

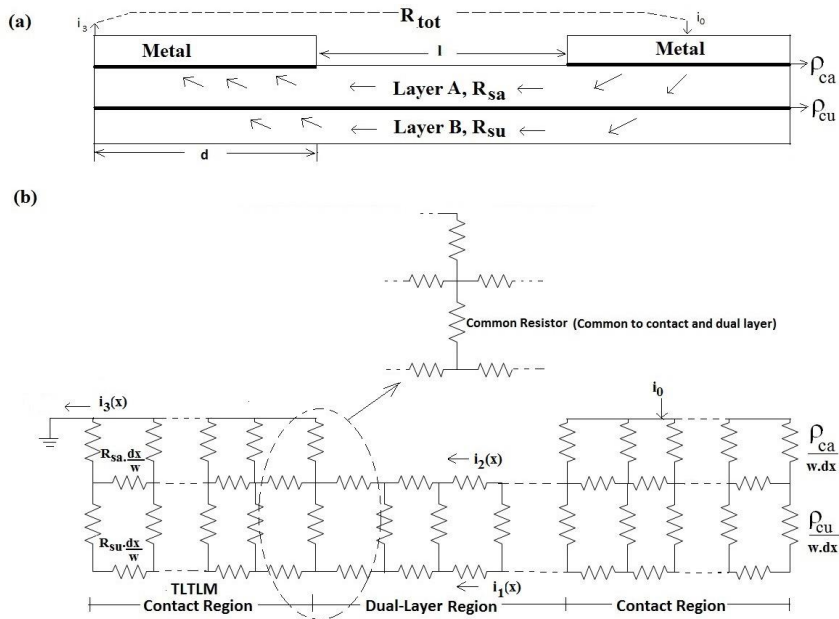


Fig. 1 Test structure for investigating resistance effects of contacts to dual-active layers. (a) Schematic of test structure and (b) resistor network model showing the TLTLM [6] contact model connected to the dual active layer model [9]. The one resistor that is common to the resistor network of both analytical models is indicated

2. METHODOLOGY

The general tri-layer contact structure investigated in this work is illustrated diagrammatically with its three layers, namely a metal layer, an intermediary active layer A and a bottom active layer B in Fig.1. The metal layer is an ideal metal layer for TLM models where the metal is at an equipotential. The FEM model considers this by making the metal in the FEM metal have the same effect by having extremely low resistivity, so it is effectively at an equipotential. Two interfaces with associated specific contact resistances (SCR) are included in the model and these occur between the metal and layer A and layer A and B with their SCR given as ρ_{ca} and ρ_{cb} respectively. The sheet resistance of the metal at the metal-semiconductor is considered to be zero and, R_{sa} and R_{sb} are the sheet resistance of layer A and B respectively. (The subscripts *-sa*, *-sb*, *-ca* and *-cb* are used to maintain uniformity in the expressions with Refs [6] and [9].) The total current given to the structure is i_0 . i_1 and i_2 represent the current in layer B and A respectively. Here, i_3 is the total current exiting through the contact. The length of the contact is d , the length between two contacts is l and w is the width of the structure. The analytical expressions for the calculation of total resistance are derived combining the Reeves' Tri-layered Transmission Line Model (TLTLM) [6] and Yao Li's Model [8].

Because the models are based on the transmission line model (TLM), (which can at best be regarded as a 2-D model) the vertical voltage dropped is not included except for the interfaces. As defined by Berger [11], the η parameter gives the ratio of voltage drop across the contact interface to the vertical voltage drop in the semiconductor layer and thus determines whether a metal and a semiconductor contact is in 3D circumstances or not (FEM is utilised in this work to investigate 3-D effects).

$$\eta = \rho_c / (\rho_b * t) \quad (1)$$

where, ρ_b and t are the resistivity and thickness of the individual semiconductor layer respectively. Consequently, the model presented in this work best suits to modelling contacts when η is typically greater than 1 because the model will be 2-D.

When the two models, dual active layer [8] and TLTLM [6] are combined to describe the test structure, the voltage drop across the common resistor (see insert in Fig.1) between two models must be the same and thus the current division factor, f can be determined by solving for voltage using this boundary condition. Reeves [9] in 1997 reported a similar structure applied to the source/drain region of a MOSFET (with a short extended dual (silicide/silicon) active layer before the contact) and considered all current entering the dual layer through layer B. In this work, we focus on the more general case of a test structure in which current enters the dual layer through both the layers as shown in Fig.1. The assumption made is that the two contacts are geometrically and electrically identical. In the following equations, f_1 is the current division factor at the intersection where current is leaving one TLTLM contact and entering the dual active layer. Factor f is the modified current division factor at the intersection of a TLTLM contact and the dual layer while current is entering the TLTLM contact from the dual active layer. Thus the boundary condition used is $i_1(x)=i_0f_1$ at $x=l$ and $i_1(x)=i_0f$ at $x=0$. The expression of modified current division, f is given by.

$$f = (E + G)/(D + F + G) \quad (2)$$

where,

$$\text{Transfer Length for the dual active layer, } \gamma = \sqrt{\frac{\rho_{cu}}{R_{sa} + R_{su}}} \quad (3)$$

$$D = \frac{\rho_{cu} \cdot \coth(l/\gamma)}{\gamma} \quad (4)$$

$$E = \frac{\rho_{cu}}{\gamma} \left(\frac{R_{sa} \cdot \cosh(l/\gamma) + (f_1(R_{sa} + R_{su}) - R_{sa})}{(R_{sa} + R_{su}) \cdot \sinh(l/\gamma)} \right) \quad (5)$$

$$F = \frac{(R_{su} - \rho_{cu} \cdot a^2) \cdot b \cdot \tanh(ad) - (R_{su} - \rho_{cu} \cdot b^2) \cdot a \cdot \tanh(bd)}{(b^2 - a^2) \cdot \tanh(bd) \cdot \tanh(ad)} \quad (6)$$

$$G = \frac{R_{sa} \cdot (b \cdot \tanh(ad) - a \cdot \tanh(bd))}{(b^2 - a^2) \cdot \tanh(bd) \cdot \tanh(ad)} \quad (7)$$

Reeves [6] demonstrated that the current ($i_l(x)$) through layer B and contact resistance (R_c) in the TLTLM are given by

$$i_1(x) = \left(\frac{i_0}{\rho_{cu} (b^2 - a^2)} \right) \cdot \left(\frac{P \cdot \sinh b(d-x)}{\sinh(bd)} - \frac{Q \cdot \sinh a(d-x)}{\sinh(bd)} \right) \quad (8)$$

$$R_c = K \cdot \left\{ \frac{P}{b \cdot \tanh(bd)} - \frac{Q}{a \cdot \tanh(ad)} \right\} \quad (9)$$

where,

$$P = f \cdot (R_{su} - \rho_{cu} \cdot a^2) - (1 - f) \cdot R_{sa} \quad (10)$$

$$Q = f \cdot (R_{su} - \rho_{cu} \cdot b^2) - (1 - f) \cdot R_{sa} \quad (11)$$

$$K = R_{su} / [\rho_{cu} \cdot w \cdot (b^2 - a^2)] \quad (12)$$

The equation for a, b and c are shown in the appendix A1, A2 and A3.

Using the work reported by Li et al. [8], the current ($i_l(x)$) through the lower layer B of the dual-layer structure and total resistance, $R_{tot}(Li)$ is given by

$$i_1(x) = i_0 \left(\frac{R_{sh}}{R_{su}} + \left(f_1 - \frac{R_{sh}}{R_{su}} \right) \frac{\sinh(\frac{l-x}{\gamma})}{\sinh(\frac{l}{\gamma})} + \left(f - \frac{R_{sh}}{R_{su}} \right) \frac{\sinh(\frac{x}{\gamma})}{\sinh(\frac{l}{\gamma})} \right) \quad (13)$$

$$R_{tot}(Li) = 2 \left(R_c + \frac{R_{sh} \beta \gamma}{2w} \right) + R_{sh} l / w \quad (14)$$

where,

$$R_{sh} = \frac{R_{su} R_{sa}}{R_{sa} + R_{su}} \quad (15)$$

$$\beta = 2 \left(\frac{f_1 + f_2}{2} \frac{R_{su}}{R_{sh}} - 1 \right) \quad (16)$$

For two contacts (in a TLM type test structure) with identical geometrical and electrical features, the total resistance, $R_{tot}(Std)$ between probes connected to each contact is usually given by

$$R_{tot}(Std) = 2R_c + R_{sh} l / w \quad (17)$$

The numerical evaluation of total resistance and current flow in all layers with different contact parameters giving various η values are shown using the table and graphs obtained from MATLAB. Also, models with similar contact parameters were simulated using Finite Element Modelling (FEM) and the results for $R_{tot}(FEM)$, $R_{tot}(Li)$ and $R_{tot}(Std)$ are compared in this work.

3. RESULTS AND DISCUSSION

The table below gives sets of contact material parameters used for analysis of the test structure of Fig. (1). The values η_a and η_u for two layers, ($\eta = \rho_c / (\rho_b * t)$), where ρ_b and t are the semiconductor layer resistivity and thickness, differs in sets due to different contact parameters. The contact length is $10\mu\text{m}$ and the length between the contacts (dual active layer) is $20\mu\text{m}$ for set 1, 2 and 3. But, the length for set 4 is $5.2\mu\text{m}$. The thickness of layers A and B are considered as 0.2 and $0.6\mu\text{m}$ respectively. The distances were chosen as being typical of a TLM type test structure. The value came about because of the mesh density used, which was the same for all models.

Table 1 Contact Parameters for the test structure

Set	$R_{sa}(\Omega/\text{sq})$	$R_{su}(\Omega/\text{sq})$	ρ_{ca} ($\Omega.\text{cm}^2$)	ρ_{cu} ($\Omega.\text{cm}^2$)	l (μm)	η_a	η_u	R_{tot} (<i>FEM</i>)	R_{tot} (<i>Li</i>)	R_{tot} (<i>Std</i>)
1	40	60	8.0E-7	1.6E-6	20	50	7	576.1	575.7	587.8
2	30	40	8.0E-7	9.0E-6	20	66.67	62.50	445.9	445.4	482.9
3	40	60	8.0E-9	1.0E-8	20	0.50	0.04	487.4	507.8	507.7
4	40	60	8.0E-7	1.6E-6	5.2	50	7	220.8	220.1	232.4

The analytical and FEM results are in excellent agreement for sets when the η value is greater than 1. Moreover, the error percentage is less between $R_{tot}(FEM)$ and $R_{tot}(Li)$ results compared to $R_{tot}(Std)$. This clearly shows that the redistribution of current near the intersection of TLTLM and the dual layer affects the total resistance between the contacts.

In sets 1 and 2, $R_{tot}(FEM)$ and $R_{tot}(Li)$ are practically the same and the error percentage is less than 1 in both cases (considering the FEM model to give the most realistic result). However, the error is 2% between $R_{tot}(FEM)$ and $R_{tot}(Std)$ for set 1 and it increased to 8% for set 2. This is because the transfer length in the dual active layer is longer for set 2 than set 1. The distance before at the leading edge of the contact that is affected by the redistribution of current due to the contact is directly proportional to the transfer length of the dual active layer. Consequently, the total resistance in the dual layer of the test structure will be different to $R_{sh} * l/w$ (where R_{sh} is the effective sheet resistance of the two parallel active layers). In set 3, both $R_{tot}(Std)$ and $R_{tot}(Li)$ have approximately 4% disagreement with the FEM results. In set 4, all the parameters are the same as set 1 except that the length between the contacts is $5.2\mu\text{m}$. As the dual active layer is shorter, and the transfer lengths do not change, the effect of the contacts on current distribution in the dual layer is relatively bigger. The error is ~5% between $R_{tot}(FEM)$ and $R_{tot}(Std)$ and less than 1% with $R_{tot}(Li)$. Thus, the expressions described in this work can give an accurate insight into the electrical behaviour of the test structure, provided that $\eta > 1$.

The graph plotted below in Fig. 2(a) is for set 1 and the point of contact for TLTLM and dual layer is considered to be point 0. The length of the TLTLM contact region is $10\mu\text{m}$ and the dual layered region is $20\mu\text{m}$. It shows the flow of current starting from the point at which current exits one TLTLM contact and enters the dual layer. Here, i_1 (solid line) is the current flowing in layer B, i_2 (dotted line) in layer A and i_3 (fine dotted line) represents the total current in the TLTLM contact. The graph illustrates that i_1 distributes itself and tends to remain constant at a ratio of $R_{sa} : R_{su}$ (i.e. $i_1 : i_2 = 4 : 6$) in the dual layered structure. But, the flow is disturbed near the point when current enters the TLTLM structure from the dual layer.

The FEM result confirms the same as shown in Fig. 2(b). The voltage contour is uniform at the middle of the dual layer, and the contour is disturbed near the TLTLM contact region.

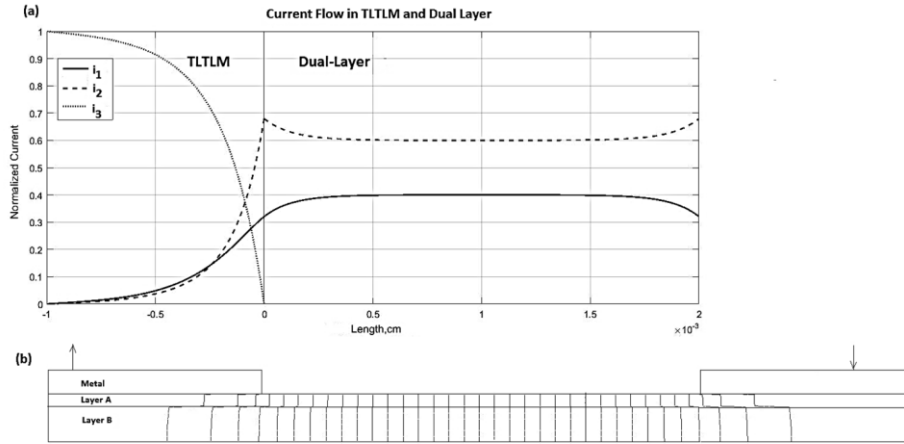


Fig. 2 (a) Current distribution in one TLTLM contact and dual layer contact regions for a test structure with $R_{sa}=40 \Omega/\text{sq}$, $R_{su}=60 \Omega/\text{sq}$, $\rho_{ca}=8e-7 \Omega \cdot \text{cm}^2$, $\rho_{cu}=1.6e-6 \Omega \cdot \text{cm}^2$ with dual active layer of $20 \mu\text{m}$ (b) distribution of corresponding voltage contours, determined by FEM for the test structure

Fig. 3(a) shows results for set 4 when all the other parameters are same as set 1 except the length between the contacts is reduced to $5.2 \mu\text{m}$. Because of this, the current flow with ratio $R_{sa}:R_{su}$ is over a shorter length. This leads to greater variation in total resistance. The higher error value of $\sim 5\%$ between $R_{tot}(Std)$ and $R_{tot}(FEM)$ shows that the total resistance between contacts is not given by $R_{sh} \cdot l/w$.

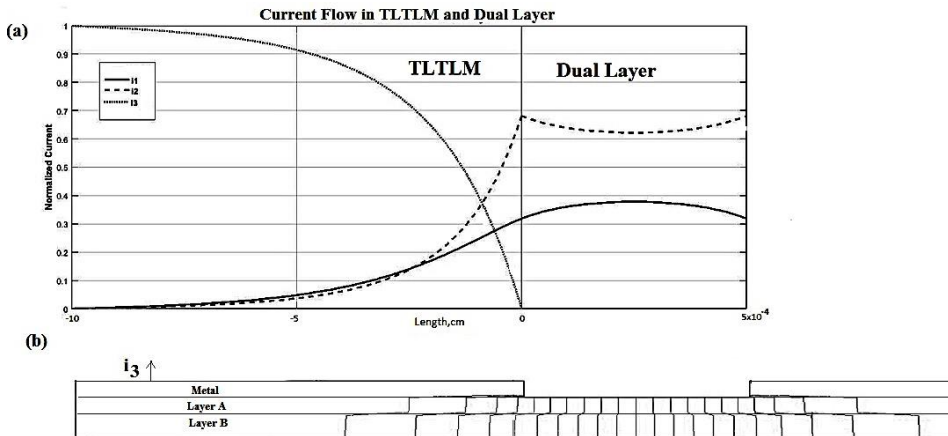


Fig. 3 (a) Current distribution in a TLTLM contact and dual layer contact regions for a test structure with $R_{sa}=40 \Omega/\text{sq}$, $R_{su}=60 \Omega/\text{sq}$, $\rho_{ca}=8e-7 \Omega \cdot \text{cm}^2$, $\rho_{cu}=1.6e-6 \Omega \cdot \text{cm}^2$ with a dual active layer of $5.2 \mu\text{m}$ in length (b) distribution of corresponding voltage contours, determined by FEM for the test structure

4. CONCLUSION

Two variations of Transmission Line Model networks, namely Tri-Layer TLM and a dual layer network, for modelling current in semiconductor contact regions, were combined to model a test structure with multiple layers. A comparison of the mathematical analysis and a two-dimensional finite element model of the test structure with two metal contacts to a dual-active layer, show that the combination of TLTLM and the dual-layer network expressions provides accurate analysis for these test structures. The limitations on the accuracy of expressions have been presented in terms of the η parameter. The distribution of current through the dual-layer and TLTLM contact region is discussed in detail to understand its influence on the total resistance of the test structure. This distribution is accurately represented by the combined TLTLM-dual-active layer model investigated which is an improvement on models where the current distribution and sheet resistance is considered uniform between contacts.

REFERENCES

- [1] A. M. Collins, Y. Pan, A. S. Holland, "Using a Two-contact circular test structure to determine the specific contact resistivity of contacts to bulk semiconductors", *Facta Universitatis, Electronics and Energetics*, vol. 28, no. 3, September 2015, pp. 457-464.
- [2] Y. Pan, A. M. Collins and A. S. Holland, "Determining Specific Contact Resistivity to Bulk Semiconductor Using a Two-Contact Circular Test Structure", In Proceedings of the IEEE International Conference on MIEL, May 2014, pp. 257-260.
- [3] V. Gudmundsson, P. Hellstrom, and M. Ostling, "Error propagation in contact resistivity extraction using cross-bridge Kelvin resistors," *IEEE Trans. Electron Devices*, vol. 59, no. 6, pp. 1585–1591, June 2012.
- [4] A. S. Holland, G. K. Reeves, "New Challenges to the Modelling and Electrical Characterisation of ohmic contacts for ULSI devices", In Proc. of the 22nd International Conference on Microelectronics (MIEL 2000), vol. 2, Niš, Serbia, pp. 461-464, 2000.
- [5] W. Shockley, "Research and Investigation of inverse epitaxial UHF power transistors", Air Force Atomic Laboratory, Wright-Patterson Air Force Base, Rep. No. AL-TDR-64-207, Sept. 1964.
- [6] G. K. Reeves, H. B. Harrison, "An analytical model for alloyed ohmic contacts using a Tri-layer Transmission Line Model", *IEEE Trans. Electron Devices*, vol. 42, no. 8, p. 1536. 1995.
- [7] G. K. Reeves, A. S. Holland, P.W. Leech, "Influence of Via Liner Properties on the Current Density and Resistance of Vias", In Proc. of the 23rd International Conference on Microelectronics (MIEL 2002), vol. 2, Niš, Yugoslavia, pp. 535-538, 2002.
- [8] Y. Li, G. K. Reeves, H. B. Harrison, "Correcting separating errors related to contact resistance measurement", *Microelectronics Journal*, vol. 29, 1996.
- [9] G. K. Reeves, H. B. Harrison, "Using TLM principles to determine MOSFET contact and parasitic resistance", *Solid-State Electronics*, vol. 41, no.8, 1997.
- [10] Y. Shiraishi, N. Furuhashi, A. Okamoto, "Influence of metal/n-InAs/interlayer/n-GaAs structure on nonalloyed ohmic contact resistance", *Journal of Applied Physics*, vol. 76, p. 5099, 1994.
- [11] H. H. Berger, "Models for contacts to planar devices", *Solid State Electronics*, vol. 12, 1972.

APPENDIX

The expressions for the TLTLM

$$a = \sqrt{\left[\frac{\{c - \sqrt{(c^2 - 4R_{su}R_{sa})/(\rho_{cu}\rho_{ca})}\}}{2} \right]} \quad (A1)$$

$$b = \sqrt{\left[\frac{\{c + \sqrt{(c^2 - 4R_{su}R_{sa})/(\rho_{cu}\rho_{ca})}\}}{2} \right]} \quad (A2)$$

$$c = \frac{R_{sa} + R_{su}}{\rho_{cu}} + \frac{R_{sa}}{\rho_{ca}} \quad (A3)$$

MATLAB CODE

%Calculation of f factor

```

Rs=Rsa+Rsu;
Rsh=(Rsu*Rsa)/(Rsu+Rsa);
al=sqrt(Rs/pcu);
c=(Rs/pcu)+(Rsa/pca);
z=sqrt((c*c)-(4*Rsu*Rsa/(pcu*pca)));
a=sqrt((c-z)/2);
b=sqrt((c+z)/2);
D=al*pcu*coth(al*1);
E=al*pcu*(Rsa*cosh(al*1)+(f1*Rs-Rsa))/(Rs*sinh(al*1));
H=((b*((Rsu-(pcu*a*a))*tanh(a*d)))-(a*((Rsu-(pcu*b*b))*tanh(b*d)))/((b*b-
a*a)*tanh(b*d)*tanh(a*d));
G=Rsa*(b*tanh(a*d)-a*tanh(b*d))/((b*b-a*a)*tanh(b*d)*tanh(a*d));
f2=(E+G)/(D+H+G);

```

% Current Flow Dual Active Layer

```

A=Rsh/Rsu;
Y1=sqrt(pcu/(Rsu+Rsa));
i11=i0*(A+((f2-A)*sinh((1-x)/Y1)/sinh(l/Y1))+((f1-A)*sinh(x/Y1)/sinh(l/Y1)));
i21=i0-i11;

```

% Current Flow TLTLM Contact

```

c=((Rsa+Rsu)/pcu)+(Rsa/pca);
z=(c*c)-(4*Rsu*Rsa)/(pcu*pca);
a=sqrt((c-sqrt(z))/2);
b=sqrt((c+sqrt(z))/2);
P=f2*(Rsu-pcu*a*a)-(1-f2)*Rsa;
Q=f2*(Rsu-pcu*b*b)-(1-f2)*Rsa;
i12=(i0/(pcu*(b*b-a*a)))*(P*sinh(b*(d+y))/sinh(b*d)-(Q*sinh(a*(d+y))/sinh(a*d)));
i23=(i0/(Rsa*pcu*(b*b-a*a)))*(P*(Rsu-pcu*b*b)*sinh(b*(d+y))/sinh(b*d)-(Q*(Rsu-
pcu*a*a)*sinh(a*(d+y))/sinh(a*d)));
itot=i0-(i12+i23);
plot(x,i11);
hold on;
plot(y,i12);
hold on;
plot(x,i21);
hold on;
plot(y,i23);
hold on;
plot(y,itot);

```

% Contact Resistance

```

c1=((Rsa+Rsu)/pcu)+(Rsa/pca);
z1=(c1*c1)-(4*Rsu*Rsa)/(pcu*pca);
a1=sqrt((c1-sqrt(z1))/2);
b1=sqrt((c1+sqrt(z1))/2);
K1=Rsu/(pcu*w*(b1*b1-a1*a1));

```

```

X1=tanh(b1*d);
Y1=tanh(a1*d);
P1=f2.*(Rsu-(pcu.*a1.*a1));
Q1=f2.*(Rsu-(pcu.*b1.*b1));
k1=(1-f2).*Rsa;
Rc=K1.*(((P1-k1)/(b1.*X1))-((Q1-k1)/(a1.*Y1)));
% Total Resistance using standard Formula
Rtot=2*Rc+(Rsh*l/w)
% Total Resistance using Yao et al. Formula when dual layer is longer
beta=2.*(((f1+f2)*Rsu)/(2*Rsh))-1;
bcor=(Rsh*beta)/(w*a1);
Rtotli=2*(Rc+(bcor/2))+(Rsh*l)/w;

```